

M1 macrophage-derived exosomes inhibit myocardial regeneration.

Xiaoqing He

Department of Cardiology, Guangzhou Institute of Cardiovascular Disease, Guangdong Key Laboratory of Vascular Diseases, The Second Affiliated Hospital, Guangzhou Medical University, Guangzhou 510260, People's Republic of China

Jing Chen

Department of Cardiology, Guangzhou Institute of Cardiovascular Disease, Guangdong Key Laboratory of Vascular Diseases, The Second Affiliated Hospital, Guangzhou Medical University, Guangzhou 510260, People's Republic of China

Jian Shi

Department of Cardiology, Guangzhou Institute of Cardiovascular Disease, Guangdong Key Laboratory of Vascular Diseases, The Second Affiliated Hospital, Guangzhou Medical University, Guangzhou 510260, People's Republic of China

Yichao Deng

Department of Cardiology, Guangzhou Institute of Cardiovascular Disease, Guangdong Key Laboratory of Vascular Diseases, The Second Affiliated Hospital, Guangzhou Medical University, Guangzhou 510260, People's Republic of China

Weihua Liu

Department of Cardiology, Guangzhou Institute of Cardiovascular Disease, Guangdong Key Laboratory of Vascular Diseases, The Second Affiliated Hospital, Guangzhou Medical University, Guangzhou 510260, People's Republic of China

Shaojun Liu

Department of Cardiology, Guangzhou Institute of Cardiovascular Disease, Guangdong Key Laboratory of Vascular Diseases, The Second Affiliated Hospital, Guangzhou Medical University, Guangzhou 510260, People's Republic of China <https://orcid.org/0000-0001-7895-5577>

Shiming Liu (✉ liushiming@gzhmu.edu.cn)

Department of Cardiology, Guangzhou Institute of Cardiovascular Disease, Guangdong Key Laboratory of Vascular Diseases, The Second Affiliated Hospital, Guangzhou Medical University, Guangzhou 510260, People's Republic of China <https://orcid.org/0000-0001-5177-1858>

Research Article

Keywords: M1 macrophage, exosomes, miR-155, myocardial regeneration, cardiac repair

Posted Date: March 28th, 2022

DOI: <https://doi.org/10.21203/rs.3.rs-1440380/v1>

License:  This work is licensed under a Creative Commons Attribution 4.0 International License.

[Read Full License](#)

Abstract

M1 macrophages inhibit cardiac repair, but their role in myocardial regeneration remains unclear. In this study, the underlying mechanisms of M1 macrophage-derived exosomes (M1-Exos) in cardiomyocyte proliferation was investigated. Mouse RAW264.7 macrophages were cultured and induced into M1 macrophages. The exosomes from the culture media of M1 macrophages were isolated, and results showed that M1-Exos could inhibit the proliferation of cardiomyocytes. During M1-Exos, miR-155 was highly expressed and delivered to the cardiomyocytes. Furthermore, miR-155 inhibited the proliferation of cardiomyocytes and antagonized the pro-proliferation effect of IL-6 via inhibition of its novel target gene IL-6R. M1-Exos inhibited cardiomyocyte proliferation and cardiac repair by delivering miR-155, which targeted IL-6R, and inhibiting the IL-6R/Jak/Stat signaling pathway. This study provides new insights and potential treatment strategies for the regulation of myocardial regeneration and cardiac repair by M1-Exos.

Introduction

Acute myocardial infarction (AMI) is an arterial obstruction caused by coronary atherosclerosis, and it could lead to myocardial ischemia, hypoxia, and irreversible myocardial injury. Some cases of AMI develop into chronic heart failure due to poor recovery of microvascular function and cardiac function [1].

Some fish and amphibians maintain the ability of cardiac regeneration throughout their lives. Newborn mice also have cardiac regeneration ability, but this talent is lost after one week of birth [2] due to cell cycle arrest [3]. Adult cardiomyocytes proliferate at a low rate of 1% per year, whereas with the increase in age, the myocardial regeneration rate continues to decline to 0.45% [4]. However, myocardial infarction is prone to occur in middle-aged and elderly people. At this time, the myocardial regeneration rate is low, and the means of cardiac repair is almost fibrosis. With the increase in adverse ventricular remodeling, the cardiac function decreases remarkable. Elucidating the underlying mechanisms of myocardial regeneration is undoubtedly necessary to promote cardiac repair and functions after myocardial infarction.

During embryonic and fetal development in rodents, cardiac growth mainly results from the increased number of the cardiomyocyte caused by the division and proliferation of immature cardiomyocytes. However, after 7 days postnatal, the enlargement of cardiomyocyte size is the primary mechanism in rodent heart growth [5]. Nonetheless, some cardiomyocytes from adult mice could re-enter the cell cycle for cell proliferation after stimulation [6]. Senyo et al. tracked the proliferation of cardiomyocytes by multi-isotope imaging mass spectrometry and found that cardiomyocytes in adult mice retained a certain regenerative capacity, and the regenerated cardiomyocytes were mainly derived from cardiomyocytes rather than stem cells [7].

After myocardial infarction, macrophages tend to the infarcted area and participate in the repair of damaged tissue [8]. Macrophages could be divided into M1 macrophages and M2 macrophages. M1

macrophages mainly play a role in removing damaged cells and their debris, while M2 macrophages mainly play a role in tissue repair [9]. Studies have shown that macrophages could inhibit cardiac repair by promoting collagen deposition in scars, forming irreversible scars and promoting fibrotic healing after myocardial infarction [10]. Inhibition of M1 macrophages and promotion of polarization to M2 macrophages could reduce adverse ventricular remodeling after myocardial infarction and improve cardiac function [11]. However, the specific mechanism of M1 macrophages inhibiting cardiac repair and the effect on cardiomyocyte proliferation still need to be further explored.

Exosomes are extracellular vesicles with a diameter of 30–200 nm, and they are rich in proteins, lipids, and nucleic acids. They have the functions of mediating intercellular communication, antigen presentation, and cell migration and differentiation [12]. Exosomes also play an important role in paracrine and autocrine signaling; for example, cardiomyocyte-derived exosomes could regulate myocardial regeneration and cardiac repair by delivering miR-21 [13]. In a previous study of the authors, M1-Exos was found to inhibit the proliferation and migration of endothelial cells, thereby further aggravating myocardial injury and inhibiting cardiac repair [14]. In the present study, the role of M1-Exos carrying miRNA in cardiomyocyte proliferation was observed, and its specific molecular mechanism, which could provide novel understanding and potential treatment strategy for myocardial infarction, was explored.

Material And Method

Reagent

RAW 264.7 mouse macrophages (SCSP-5036) were provided by the Chinese Academy of Sciences. Dulbecco's modified Eagle medium (DMEM, C11995500BT), penicillin-streptomycin (15140122), collagenase type II (17101015), trypsin (25200072), and Lipofectamine 3000 transfection kit were purchased from Thermo Fisher Scientific. GM-CSF (51048-MNAH) and IFN- γ (50709-MNAH) were purchased from Sino Biological. Exosome-depleted fetal bovine serum (C3801-0050) was provided by VivaCell BIOSCIENCES. Fetal bovine serum (1913444) was provided by Biological Industries. Antibodies, including anti-CD63 (ab193349), phalloidin-iFluor 488 (ab176753), and anti-CD9 (ab92726), were purchased from abcam, and calnexin polyclonal antibody (10427-2-AP) was purchased from proteintech. Antibodies, including phospho-histone H3 (9713), ki-67 (9129), α -actinin (69758), phospho-Jak2 (3771), phospho-Stat3 (9145), and GAPDH (5174), were all purchased from Cell Signaling Technology. Antibodies, including anti-CD81 (sc-166029) and anti-IL-6R α (sc-373708), were purchased from Santa Cruz Biotechnology. Peroxidase AffiniPure goat anti-mouse IgG (115-035-003) and peroxidase AffiniPure goat anti-rabbit IgG (111-035-003) were purchased from Jackson ImmunoResearch. Small interfering RNA (siRNA) was purchased from Genescript.

Small interfering RNA		
Negative control	sense	UUCUCCGAACGUGUCACGUTT
	antisense	ACGUGACACGUUCGGAGAATT
mmu-miR-155 mimic	sense	UUA AUGCUAAUUGUGAUAGGGGU
	antisense	CCCUAUCACAAUUAGCAUUAUU

Mice and MI model

Male C57BL/6J mice aged 8–10 week were purchased from Guangzhou Dean Gene Technology Co., Ltd. and bred in the Animal Center of the Second Affiliated Hospital of Guangzhou Medical University. C57BL/6J mice aged 1–3 days were purchased from Guangzhou University of Chinese Medicine. All animal projects complied with the National Institutes of Health Guide for the Care and Use of Laboratory Animals, and they were approved by the Animal Care and Use Committee of Guangzhou Medical University (Ethics Number: 2019-014).

Mice were anesthetized with 2% isoflurane and connected to a small animal ventilator. The heart was exposed at the left third rib of the chest, and the left anterior descending coronary artery was ligated with 9 – 0 polyester suture. The anterior wall of the left ventricle became white, and the periapical beat weakened.

Induction of M1 macrophages

After the macrophages were grown to a density of 60–70%, the M0 macrophage group was added with DMEM containing 5% exosome-depleted FBS, while the M1 macrophage group was added with DMEM containing 5% exosome-depleted FBS, mouse GM-CSF (50ng/mL) and mouse IFN- γ (20ng/mL) for 24 h.

Culture and treatment of primary cardiomyocytes

The hearts of C57BL/6 neonatal mice aged 1–3 days were taken out and placed in pre-cooled PBS, and the atrial appendages and atria were removed to preserve the ventricles. The ventricular tissue was torn and pressed into thin tissue pieces, which were digested with 0.125% trypsin at 4°C for 12–13 h. An appropriate amount of collagenase II digestion solution was added, and the mixture was shaken and digested in 37°C water bath for 8 min. It was quickly and vigorously pipetted until no obvious tissue could be observed, and then the mixture was shaken and digested again for 8 min. It was vigorously pipetted until no tissue was visible and then centrifuged at room temperature at 950 rpm for 3 min. An appropriate amount of DMEM with 10% FBS and 1% penicillin-streptomycin was added to resuspend the cells and placed in the incubator for 1.5 h twice (37°C, 5% CO₂, 95% air). The unattached cells were collected, centrifuged at 950 rpm for 3 min at room temperature, added with DMEM containing 10% FBS, 1% penicillin-streptomycin, and 100 μ M Brdu to resuspend the cells. Next, they were transferred to a six-well plate, mixed well, and incubated for 48 h (37°C, 5% CO₂, 95% air). The cardiomyocytes were treated with IL-6 at 50 ng/mL.

Isolation of exosomes

The medium of M0 macrophages and M1 macrophages was collected separately, and the exosomes in the medium were isolated by differential ultracentrifugation. The collected medium was centrifuged in 50 mL centrifuge tubes at 4°C for 300×*g* for 15 min, 2,000×*g* for 30 min, and 10,000×*g* for 60 min. The supernatant was transferred and centrifuged at 100,000×*g* for 90 min at 4°C. The pellets were resuspended with 10 mL of pre-cooled PBS and centrifuged again at the same speed. The pellets were exosomes, and they were resuspended in 200 μL pre-cooled PBS.

Uptake and treatment of exosomes

The operation was in accordance with Sigma's PKH26 kit instructions. Four μL of PKH26 ethanolic dye solution was added to 1 mL of Diluent C, and the exosomes was resuspended with the mixture. After 5 min of incubation at room temperature in the dark, the reaction was terminated by adding 2 mL of 0.5% BSA. An appropriate amount of medium was added, and the mixture was centrifuged twice at 100,000×*g* for 90 min at 4°C to remove unbound dye. The labeled exosomes were resuspended in DMEM containing 5% exosome-depleted FBS, added to cardiomyocytes at 2×10^9 /mL, and placed in a cell incubator (37°C, 5% CO₂, 95% air) in the dark for 10 h. After the cells were fixed with 4% paraformaldehyde, the cytoskeleton was stained with phalloidin-iFluor488 at room temperature for 30 min in the dark, and the nuclei were stained with 4',6-diamidino-2-phenylindole (DAPI) at room temperature for 10 min in the dark. After the excess antibody was washed, an anti-fluorescence quencher was added, and the uptake was observed and photographed under a laser confocal microscope.

The exosomes were isolated in accordance with step 2.5, and their particle size was calculated by nanoparticle tracking analysis (NTA). Then, the concentration of exosome resuspension was calculated. The exosomes were added to DMEM containing 5% exosome-depleted FBS at 2×10^9 /mL and co-cultured with cardiomyocytes for 24 h.

Cardiomyocyte transfection

After the cardiomyocytes adhered and grew, the cells were transfected in accordance with the instructions of Lipofectamine 3000 transfection kit. The concentration of siRNA in the negative control group and miR-155 mimic group was 100 nM, while the same amount of PBS was added in the mock group. The transfection mixture was added into the target well and incubated for 8 h. Then, the medium was changed to DMEM containing 10% FBS and 1% penicillin–streptomycin and cultured for 40 h.

Immunohistochemistry

The sections were placed in xylene I for 15 min, xylene II for 15 min, anhydrous ethanol I for 5 min, anhydrous ethanol II for 5 min, 85% alcohol for 5 min, 75% alcohol for 5 min, and distilled water for washing. Then, they were placed in a retrieval box filled with EDTA antigen retrieval buffer for antigen retrieval in a microwave oven. They were heated for 8 min to boiling, heating was stopped for 8 min, and then heating resumed for 7 min. The sections were placed in PBS and washed them three times for 5 min

after cooling. They were sealed at 3% BSA for 30 min after drying. After the primary antibody was added, the sections were placed flat in a humidified box at 4°C overnight. After washing three times with PBS, secondary antibody was added to cover the tissue, and incubated at room temperature for 50 min in the dark. The DAPI was incubated for 10 min in the same manner. A spontaneous fluorescence quenching reagent was added for 5 min and rinsed with running water for 10 min. After mounting with anti-fade mounting medium, images were observed and collected under a fluorescence microscope.

Immunocytochemistry

After soaking in 4% paraformaldehyde for 20–30 min, 0.5% TritonX-100 was added to permeabilize for 20 min at room temperature. Then, 5% BSA was blocked at room temperature for 1 h, and primary antibody was added to incubate at 4°C overnight. Incubation was performed with fluorescent secondary antibody for 1–2 h at room temperature, and then DAPI was added and incubated at room temperature for 10–15 min. Finally, images were observed and taken under a fluorescent inverted microscope.

Immunoblotting

Cells and exosome proteins were lysed on ice, and the cell membranes were disrupted by ultrasound to release the proteins. Then, they were centrifuged at 4°C at 12,000 rpm for 15 min. The protein sample concentration was measured by BCA method, and the concentrations of proteins of each group were adjusted to the same concentration. The proteins were placed at 100°C for 5 min and cooled on ice for 1 min. Subsequently, 10% gels were prepared and loaded in sequence for vertical protein electrophoresis. The amount of protein in each well was 15–30 ug. The PVDF membrane was activated with methanol and then transferred with a sandwich transfer clip. It was blocked by adding 5% nonfat dry milk and shaken slowly at room temperature for 1 h. The target band was placed into the corresponding primary antibody and incubated overnight at 4°C at 40 rpm. The corresponding secondary antibody was selected in accordance with the source of the primary antibody species and added to the corresponding target band to incubate at room temperature at 40 rpm for 1 h. After exposure and development in the darkroom, the corresponding target protein name, molecular weight, grouping, and other information were marked on the film, and the data were saved and analyzed statistically.

RNA extraction, reverse transcription, and RT-qPCR

One mL of TRIzol reagent was added to cells or exosomes and lysed for 10–15 min on ice. The cells were gently pipetted down with a sterile enzyme-free pipette tip and collected into a 1.5 mL EP tube. Then, 200 µL of chloroform was added to the lysate and shaken up and down to mix well. After standing at room temperature for 10 min, the lysate was centrifuged at 4°C for 12,000×*g* for 15 min. The liquid could be observed to be divided into three layers. It was then tilted 45°, and the upper transparent liquid was slowly pipetted into a new EP tube. Next, 500 µL of isopropanol was added, let stand at room temperature for 10 min, and centrifuged at 4°C for 12,000×*g* for 10 min. A white precipitate (RNA) could be seen at the bottom. Afterwards, 1 mL of pre-cooled 75% ethanol was added, the precipitate was dissolved, and centrifugation was performed at 4°C for 7500×*g* for 5 min. After air drying was conducted for 5–10 min, an appropriate amount of DEPC was added to resuspend the RNA, and a microplate reader was used to

measure the RNA absorbance (A_{260/280}) and concentration. Reverse transcription and RT-qPCR were performed in accordance with the instructions of TaKaRa's Prime Script RT reagent kit (Perfect Real Time) and TB Green Premix Ex Taq II (Tli RNaseH Plus) kit.

Dual luciferase reporter assays

When the growth density of HEK293T cells reaches approximately 50–60%, co-transfection of siRNA and plasmids was carried out following the instructions of Lipofectamine 3000 reagent. The siRNA of the negative control and miR-155 mimic were transfected at 20 nM, while plasmids were transfected at 150 ng. The transfection mixture was added to the corresponding groups and placed in an incubator for 6–8 h, and then the medium was replaced with DMEM containing 10% FBS and 1% penicillin–streptomycin for another 40 h. The cells were removed, and the operation was performed in accordance with the instructions of the dual luciferase reporter assay kit. First, 65 μ L of prepared 1 \times PLB was added to the cells, which were then shaken slowly at room temperature for 15 min. Next, the cell lysate was collected, and 50 μ L of prepared LAR II and 10 μ L of cell lysate were added to the detection tube. Afterwards, the firefly fluorescence value was measured using the detector and recorded as Read1. After the detection, 50 μ L of 1 \times Stop & Glo was added to the detection tube and mixed well to detect the fluorescence value of Renilla immediately. The fluorescence value of Renilla, recorded as Read2, was used as an internal reference for data analysis with Read1/Read2.

Statistical analysis

Statistical analysis of data was performed on GraphPad Prism 8.0 software, and all data are expressed as mean \pm standard error. Comparisons between two groups were performed using T test, and comparisons between multiple groups were performed using one-way ANOVA or two-way ANOVA. If statistical significance was found, the Bonferroni method was used for further statistical analysis, and the difference was considered to be statistically significant when $P < 0.05$.

Result

Induction and identification of M1-Exos

The M0 and M1 macrophage exosomes were isolated in accordance with differential ultracentrifugation. The particle size and concentration of the isolated exosomes were measured by NTA, and the results showed that almost all particles were between 77 and 200 nm in size, with a peak at 133 nm (Fig. 1A). Meanwhile, the morphology of the isolated exosomes was observed by transmission electron microscopy (TEM). The size of exosome particles was approximately 100–150 nm, and they were saucer-like vesicles (Fig. 1B). The biomarkers of exosomes and cell phenotypes were also compared by immunoblotting, and the results showed that CD81 and CD63, as marker proteins of exosomes, were only expressed in M0 and M1 macrophage exosomes. Calnexin, a protein derived from the endoplasmic reticulum, and the macrophage marker protein CD68 were only expressed in M0 and M1 macrophages (Fig. 1C). The

morphology, particle size, and immunoblotting results of the precipitated particles were consistent with the characteristics of exosomes.

M1-Exos inhibited cardiomyocyte proliferation

Primary cardiomyocytes were treated with the labeled M1-Exos, and their uptake was observed under a confocal laser microscope. PKH26-labeled macrophage-derived exosomes (red) were observed in cardiomyocytes and accumulated around the nucleus (Fig. 2A), suggesting primary cardiomyocytes could take up macrophage-derived exosomes.

Cardiomyocyte proliferation treated with macrophage-derived exosome was also observed to evaluate the effect of M1-Exos on the regulation of myocardial regeneration. Compared with the mock and the M0-Exos groups, the number of positive cells for both phospho-histone H3 and ki67 markers in cardiomyocytes was significantly reduced (Fig. 2B). This finding indicated that M1-Exos inhibited the proliferation of cardiomyocytes.

M1-Exos delivered miR-155 to cardiomyocytes

The previous study showed high expression of miR-155 in M1-Exos [14]. The present study yielded similar results. The expression of miR-155 in M1 macrophages and M1-Exos was higher than that in M0 macrophages and M0-Exos (Fig. 3A). The expression of miR-155 in cardiomyocytes treated with exosomes was significantly increased compared with that in the mock and the M0-Exos groups (Fig. 3B), suggesting M1 macrophages and M1-Exos were rich in miR-155 and carried miR-155 to primary cardiomyocytes.

miR-155 inhibited myocardial regeneration

To test the effect of miR-155 on cardiomyocytes proliferation, miR-155 was transfected into cardiomyocytes. Compared with that in the mock and the negative control groups, the number of cardiomyocytes marked by phospho-histone H3 or ki67 in the miR-155 group was significantly reduced (Fig. 4A). Furthermore, miR-155-carrying adenovirus was injected into the peri-infarct tissue to observe myocardial regeneration. After MI, the number of cardiomyocytes marked by phospho-histone H3 in the miR-155 group was significantly reduced compared with that in the MI and negative control groups (Fig. 4B). The data demonstrated that miR-155 inhibited cardiomyocyte proliferation and myocardial regeneration.

miR-155 targeted IL-6R

Bioinformatics analysis was performed to elucidate the specific molecular mechanism by which miR-155 inhibits cardiomyocyte proliferation, and IL-6R was predicted as a potential target gene of miR-155 (Fig. 5A). The dual luciferase reporter assays confirmed that miR-155 could significantly inhibit the WT 3' -UTR of IL-6R but not the mutant 3' -UTR (Fig. 5B). Further, the mRNA level (Fig. 5C) and protein

expression (Fig. 5D) of IL-6R in the cardiomyocytes transfected with miR-155 were decreased compared with those in the mock and negative control groups. These results indicated that IL-6R is a direct target gene of miR-155.

miR-155 antagonized IL-6-induced cardiomyocyte proliferation by inhibiting IL6/IL-6R/Jak/Stat pathway

IL-6 is required for cardiomyocyte proliferation and cardiac repair [15]. Here, whether IL-6-induced cardiomyocyte proliferation was regulated by miR-155 was explored. Compared with that in the control group, the number of cardiomyocytes marked by phospho-histone H3 or ki67 in the IL-6 treatment group was significantly increased, which verified the pro-proliferation effect of IL-6 on cardiomyocytes (Fig. 6A).

In addition, compared with the negative control group, miR-155 significantly decreased IL-6-induced cardiomyocyte proliferation (Fig. 6B). IL-6 could also increase the levels of IL-6R, phospho-Jak2, and phospho-Stat3, while miR-155 antagonized this effect of IL-6 (Fig. 6C). Therefore, miR-155 antagonized IL-6-induced cardiomyocyte proliferation by inhibiting the IL-6R/Jak/Stat pathway.

Discussion

After myocardial infarction, 25% of cardiomyocytes could be damaged in a short time, but cardiomyocytes hardly regenerate, and the lack of cardiomyocytes is the main reason for poor ventricular remodeling [16]. Therefore, the mechanism of regulating myocardial regeneration is particularly important for cardiac repair after myocardial infarction. Understanding the specific mechanism of myocardial regeneration could fill the current gap on how to regulate myocardial regeneration and change the view that cardiomyocytes are not regenerable. In the early inflammatory stage after myocardial infarction, a large number of inflammatory cells accumulates in the infarcted site, and monocytes differentiate into macrophages, which could be polarized into M1 macrophages and M2 macrophages. M1 macrophages are mainly pro-inflammatory, and they play the role of rapidly removing damaged tissues and cells. Meanwhile, M2 macrophages are mainly anti-inflammatory, and they play a role in repairing damaged tissues and improving ventricular remodeling [9]. Therefore, M1 macrophages may play an inhibitory role in cardiac repair after myocardial infarction, while anti-inflammatory M2 macrophages are often considered to have functions, such as promoting angiogenesis, cell proliferation, and tissue repair [17]. Regulating the balance switch between pro-inflammatory M1 macrophages and anti-inflammatory M2 macrophages may affect the inflammatory response at the site of myocardial infarction, thereby regulating the process of cardiac repair. Ramanujam's study showed that M1 macrophages could promote the transition of fibroblasts to myofibroblasts and promote cardiac fibrosis repair [18]. Kim et al. showed that the appropriate conversion of M1 macrophages to M2 macrophages could promote the function of collagen deposition and endothelial cell tubule formation, and accelerate wound healing [19]. The previous published studies of the authors indicated that M1 macrophages have inhibitory effects on fibroblasts [10] and endothelial cells [14]. M1-Exos could inhibit endothelial cell regeneration and its

function, and finally achieve the effect of inhibiting cardiac repair ^[14]. In the present study, M1-Exos was found to be involved in the regulation of myocardial regeneration, inhibiting cardiomyocyte proliferation and cardiac repair. M1-Exos contained a large amount of miR-155, and transfection of miR-155 mimic could inhibit the proliferation of cardiomyocytes. IL-6R was confirmed as a new target gene of miR-155 by bioinformatics analysis. miR-155 inhibited IL-6-induced cardiomyocytes proliferation by repressing the IL-6R/Jak/Stat signaling pathway.

MicroRNA (miRNA) is a new class of small non-coding RNA, and miR-155 is mainly expressed in macrophages and T cells ^[20]. It is an important regulator of immune inflammation and involved in the regulation of pathophysiological processes, such as cardiovascular disease and immune inflammation ^[21]. The expression of miR-155 was reported to be increased in mouse heart after myocardial infarction, and it could be delivered to fibroblasts in the form of exosomes, inhibiting the proliferation of fibroblasts and increasing the risk of cardiac rupture after myocardial infarction ^[22]. miR-155 also inhibited endothelial cell proliferation, tubule formation, cell migration, and other functions, thereby further inhibiting cardiac repair ^[14]. The experimental results of the present study indicated that M1-Exos is rich in miR-155 and could deliver miR-155 to cardiomyocytes, thereby inhibiting cardiomyocyte proliferation. Therefore, miR-155 regulates myocardial regeneration and cardiac repair after myocardial infarction, and plays an inhibitory role in them. Inhibition of miR-155 could promote the polarization of macrophages to M2 macrophages ^[23]. Maarten et al. observed that inhibition of miR-155 reduced myocardial damage during viral myocarditis, and long-term inhibition of miR-155 even improved survival and cardiac function ^[20]. Therefore, miR-155 may be an important target for the treatment of myocardial infarction, and inhibition of miR-155 may be a potential strategy for promoting myocardial regeneration and cardiac repair.

IL-6 is necessary for myocardial regeneration and cardiac repair, and the pro-proliferation effect of IL-6 on neonatal mouse cardiomyocytes is mediated by Stat3 signaling ^[15]. The Jak/Stat3 signaling pathway in the heart has multiple cellular functions, including myocardial differentiation, cell cycle re-entry after injury and anti-apoptosis under pathological conditions; thus, modulating Stat3 activity has great potential for regulating myocardial regeneration ^[24]. Fang et al. confirmed that the cardiomyocyte regeneration in zebrafish is promoted by the Jak/Stat signaling pathway, and inhibition of Stat3 expression could inhibit myocardial regeneration ^[25]. In the present study, IL-6R was predicted and confirmed to be a novel target gene of miR-155. Therefore, miR-155 was able to inhibit the IL-6R/Jak/Stat pathway. Considering that IL-6R/Jak/Stat is one of the key pathways of cardiomyocyte proliferation, miR-155 could inhibit cardiomyocyte proliferation by antagonizing the IL-6R/Jak/Stat pathway.

In conclusion, M1-Exos delivered miR-155 into cardiomyocytes after myocardial infarction, while miR-155 could inhibit the cardiomyocytes regeneration by suppressing the IL-6R/Jak/Stat pathway, thereby further inhibiting cardiac repair. This study indicated that inhibiting miR-155 may improve cardiac repair and adverse ventricular remodeling, and then restore cardiac function, which could improve the prognosis and

quality of life of patients with myocardial infarction. Therefore, miR-155 inhibitors may develop into potential drugs for clinical treatment of myocardial infarction.

Declarations

Funding

This study was supported by research grants from National Natural Science Foundation of China (No. 82170413, 81873474), Natural Science Foundation of Guangdong Province (2021A1515012546, 2021A1515011364, 2019A1515011214), and Science and Technology Program of Guangzhou, China (202102010101).

Competing Interests

Financial interests: Authors have no financial interests.

Data Availability

The datasets generated and analyzed during the current study are available from the corresponding authors upon request.

References

1. Betgem RP, de Waard GA, Nijveldt R, Beek AM, Escaned J, van Royen N (2015) Intramyocardial haemorrhage after acute myocardial infarction. *Nat Rev Cardiol* 12(3):156–167
2. Porrello ER, Mahmoud AI, Simpson E, Hill JA, Richardson JA, Olson EN, Sadek HA (2011) Transient regenerative potential of the neonatal mouse heart *Science* 331(6020):1078–1080
3. Mahmoud AI, Kocabas F, Muralidhar SA, Kimura W, Koura AS, Thet S, Porrello ER, Sadek HA (2013) Meis1 regulates postnatal cardiomyocyte cell cycle arrest. *Nature* 497(7448):249–253
4. Li M, Izpisua JC, Belmonte (2016) Mending a Faltering Heart *Circ Res* 118(2):344–351
5. Eschenhagen T, Bolli R, Braun T, Field LJ, Fleischmann BK, Frisen J, Giacca M, Hare JM, Houser S, Lee RT, Marban E, Martin JF, Molkentin JD, Murry CE, Riley PR, Ruiz-Lozano P, Sadek HA, Sussman MA, Hill JA (2017) Cardiomyocyte Regeneration: A Consensus Statement. *Circulation* 136(7):680–686
6. Malliaras K, Zhang Y, Seinfeld J, Galang G, Tseliou E, Cheng K, Sun B, Aminzadeh M, Marban E (2013) Cardiomyocyte proliferation and progenitor cell recruitment underlie therapeutic regeneration after myocardial infarction in the adult mouse heart. *EMBO Mol Med* 5(2):191–209
7. Senyo SE, Steinhauser ML, Pizzimenti CL, Yang VK, Cai L, Wang M, Wu TD, Guerquin-Kern JL, Lechene CP, Lee RT (2013) Mammalian heart renewal by pre-existing cardiomyocytes. *Nature* 493(7432):433–436

8. Frantz S, Nahrendorf M (2014) Cardiac macrophages and their role in ischaemic heart disease. *Cardiovasc Res* 102(2):240–248
9. Hao Q, Kundu S, Kleam J, Zhao ZJ, Idell S, Tang H (2021) Enhanced RIPK3 kinase activity-dependent lytic cell death in M1 but not M2 macrophages. *Mol Immunol* 129:86–93
10. Simoes FC, Cahill TJ, Kenyon A, Gavriouchkina D, Vieira JM, Sun X, Pezzolla D, Ravaut C, Masmanian E, Weinberger M, Mayes S, Lemieux ME, Barnette DN, Gunadasa-Rohling M, Williams RM, Greaves DR, Trinh LA, Fraser SE, Dallas SL, Choudhury RP, Sauka-Spengler T, Riley PR (2020) Macrophages directly contribute collagen to scar formation during zebrafish heart regeneration and mouse heart repair. *Nat Commun* 11(1):600
11. Lim GB (2018) Heart failure: Macrophages promote cardiac fibrosis and diastolic dysfunction. *Nat Rev Cardiol* 15(4):196–197
12. Pegtel DM, Gould SJ (2019) Exosomes *Annu Rev Biochem* 88:487–514
13. Qiao L, Hu S, Liu S, Zhang H, Ma H, Huang K, Li Z, Su T, Vandergriff A, Tang J, Allen T, Dinh PU, Cores J, Yin Q, Li Y, Cheng K (2019) *microRNA-21-5p dysregulation in exosomes derived from heart failure patients impairs regenerative potential*. *J Clin Invest*, **129**(6): p. 2237–2250
14. Liu S, Chen J, Shi J, Zhou W, Wang L, Fang W, Zhong Y, Chen X, Chen Y, Sabri A, Liu S (2020) *M1-like macrophage-derived exosomes suppress angiogenesis and exacerbate cardiac dysfunction in a myocardial infarction microenvironment*. *Basic Res Cardiol*, **115**(2): p. 22
15. Han C, Nie Y, Lian H, Liu R, He F, Huang H, Hu S (2015) Acute inflammation stimulates a regenerative response in the neonatal mouse heart. *Cell Res* 25(10):1137–1151
16. Laflamme MA, Murry CE (2011) Heart regeneration *Nature* 473(7347):326–335
17. Fujiu K, Wang J, Nagai R (2014) Cardioprotective function of cardiac macrophages. *Cardiovasc Res* 102(2):232–239
18. Ramanujam D, Schon AP, Beck C, Vaccarello P, Felician G, Dueck A, Esfandyari D, Meister G, Meitinger T, Schulz C, Engelhardt S (2021) MicroRNA-21-Dependent Macrophage-to-Fibroblast Signaling Determines the Cardiac Response to Pressure Overload. *Circulation* 143(15):1513–1525
19. Kim H, Wang SY, Kwak G, Yang Y, Kwon IC, Kim SH (2019) Exosome-Guided Phenotypic Switch of M1 to M2 Macrophages for Cutaneous Wound Healing. *Adv Sci (Weinh)* 6(20):1900513
20. Corsten MF, Papageorgiou A, Verhesen W, Carai P, Lindow M, Obad S, Summer G, Coort SL, Hazebroek M, van Leeuwen R, Gijbels MJ, Wijnands E, Biessen EA, De Winther MP, Stassen FR, Carmeliet P, Kauppinen S, Schroen B, Heymans S (2012) MicroRNA profiling identifies microRNA-155 as an adverse mediator of cardiac injury and dysfunction during acute viral myocarditis. *Circ Res* 111(4):415–425
21. Bala S, Csak T, Saha B, Zatsiorsky J, Kodys K, Catalano D, Satishchandran A, Szabo G (2016) The pro-inflammatory effects of miR-155 promote liver fibrosis and alcohol-induced steatohepatitis. *J Hepatol* 64(6):1378–1387
22. Wang C, Zhang C, Liu L, Chen XAB, Li Y, Du J (2017) Macrophage-Derived mir-155-Containing Exosomes Suppress Fibroblast Proliferation and Promote Fibroblast Inflammation during Cardiac

23. Zhang Y, Zhang M, Li X, Tang Z, Wang X, Zhong M, Suo Q, Zhang Y, Lv K (2016) Silencing MicroRNA-155 Attenuates Cardiac Injury and Dysfunction in Viral Myocarditis via Promotion of M2 Phenotype Polarization of Macrophages. *Sci Rep* 6:22613
24. Nakao S, Tsukamoto T, Ueyama T, Kawamura T (2020) *STAT3 for Cardiac Regenerative Medicine: Involvement in Stem Cell Biology, Pathophysiology, and Bioengineering*. *Int J Mol Sci*, 21(6)
25. Fang Y, Gupta V, Karra R, Holdway JE, Kikuchi K, Poss KD (2013) Translational profiling of cardiomyocytes identifies an early Jak1/Stat3 injury response required for zebrafish heart regeneration. *Proc Natl Acad Sci U S A* 110(33):13416–13421

Figures

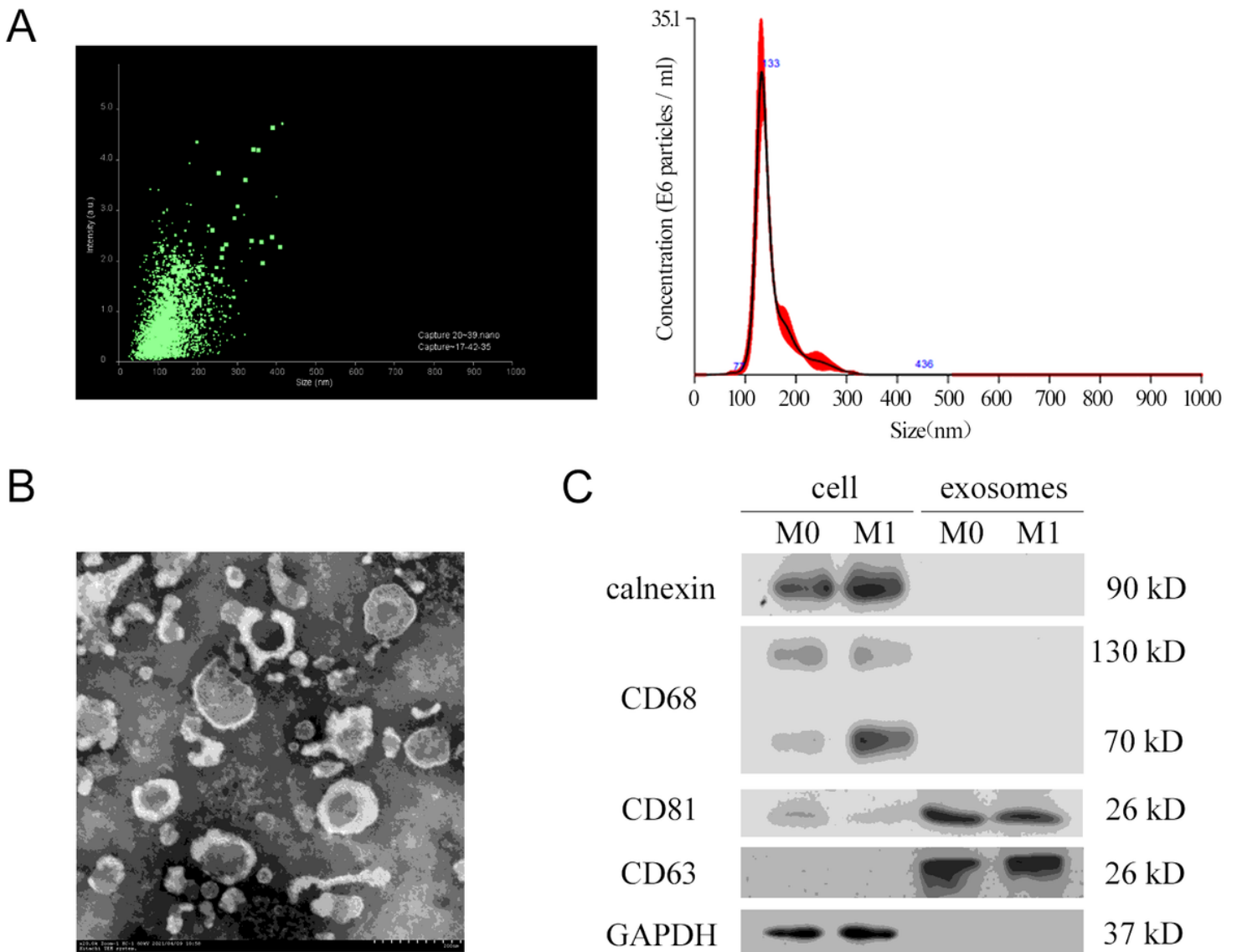


Figure 1

Induction and identification of M1-Exos

A) The particle size and concentration of isolated exosomes were detected using nanoparticle tracking analysis. B) The size and shape of macrophage-derived exosomes were observed by transmission electron microscopy. Scale bar: 200 nm. C) Immunoblotting was performed with macrophage marker proteins calnexin and CD68, and exosome marker proteins CD81 and CD63. GAPDH served as a loading control. Each experiment in this figure was replicated more than three times.

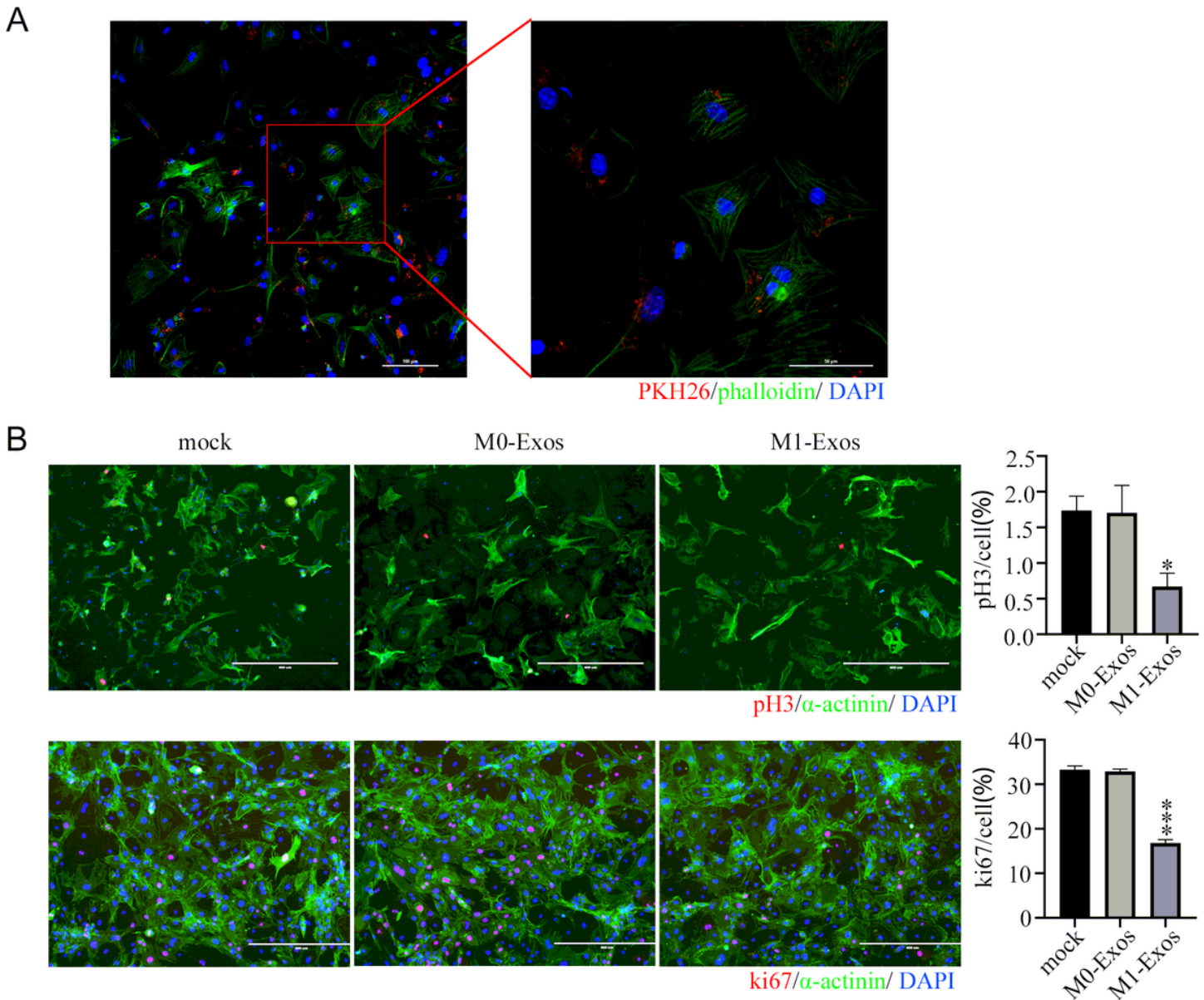


Figure 2

Inhibition of cardiomyocyte proliferation by M1-Exos

A) After PKH26-labeled exosomes (red) were added to cardiomyocytes at a concentration of 2×10^9 /mL for 10 h, the uptake of exosomes was observed by confocal laser microscopy. Scale bar: 100 μ m. B) M0-

Exos and M1-Exos were added to cardiomyocytes at a concentration of 2×10^9 /mL for 24 h, and the number of cardiomyocytes labeled with phospho-histone H3 or ki67 (red) was observed by immunocytochemistry. Scale bar: 400 μ m. Each experiment in this figure was replicated more than three times. * $P < 0.05$, *** $P < 0.001$.

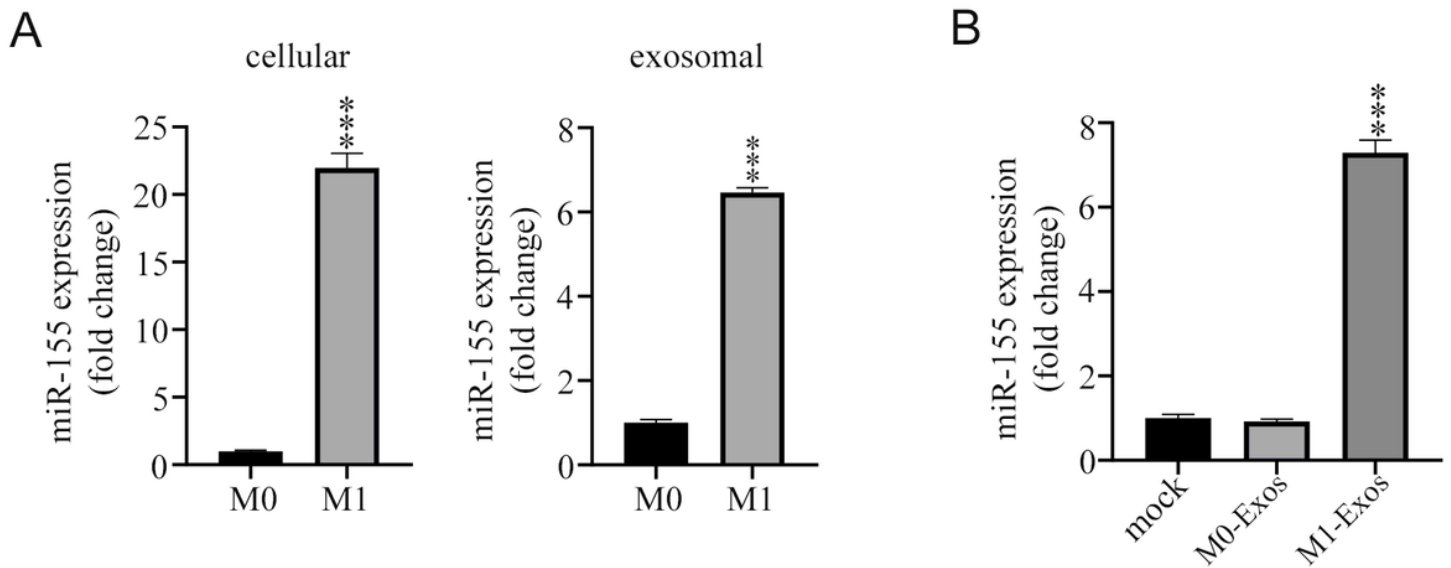


Figure 3

Delivery of miR-155 to cardiomyocytes by M1-Exos

A) M1 macrophages were treated with 50 ng/mL GM-CSF and 20 ng/mL IFN- γ for 24 h. The expression of miR-155 in cells (left) and exosomes (right) was detected by qRT-PCR. B) After M0-Exos and M1-Exos were added to cardiomyocytes at a concentration of 2×10^9 /mL for 24 h, the expression of miR-155 in cardiomyocytes was detected by qRT-PCR. Each experiment in this figure was replicated more than three times. *** $P < 0.001$.

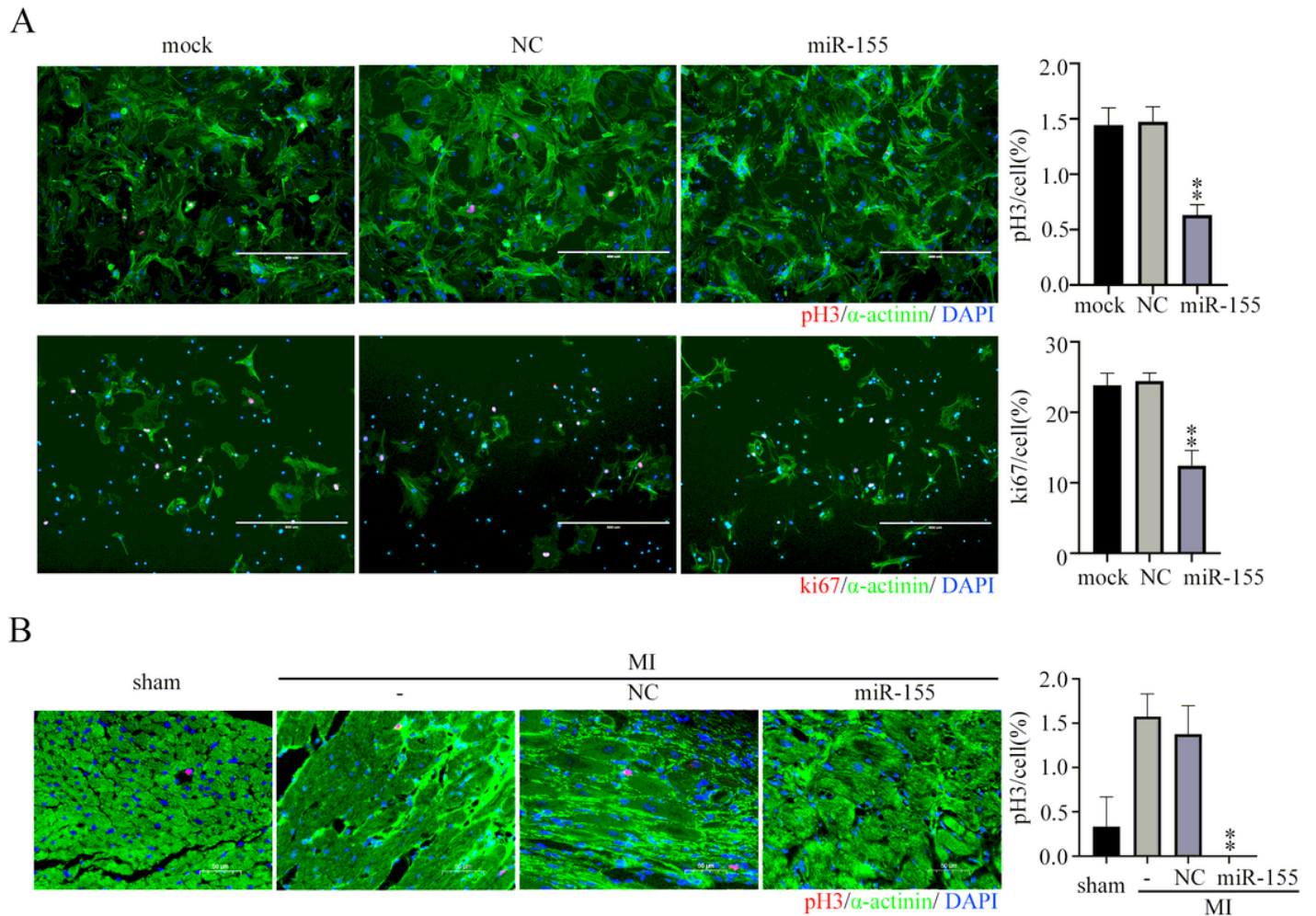


Figure 4

Inhibition of myocardial regeneration by miR-155

A) Negative control or miR-155 mimic was transfected into cardiomyocytes at 100 nM for 48 h, and the number of cardiomyocytes labeled with phospho-histone H3 or ki67 (red) was observed by immunocytochemistry. Scale bar: 400 μ m. B) After the mouse MI model was constructed, 50 μ l of miR-155 adenovirus was injected into the peri-infarct tissue. The hearts were removed for immunofluorescence after 14 days, and the number of phospho-histone H3- labeled cardiomyocytes was observed. Each experiment in this figure was replicated more than three times. ** $P < 0.01$.

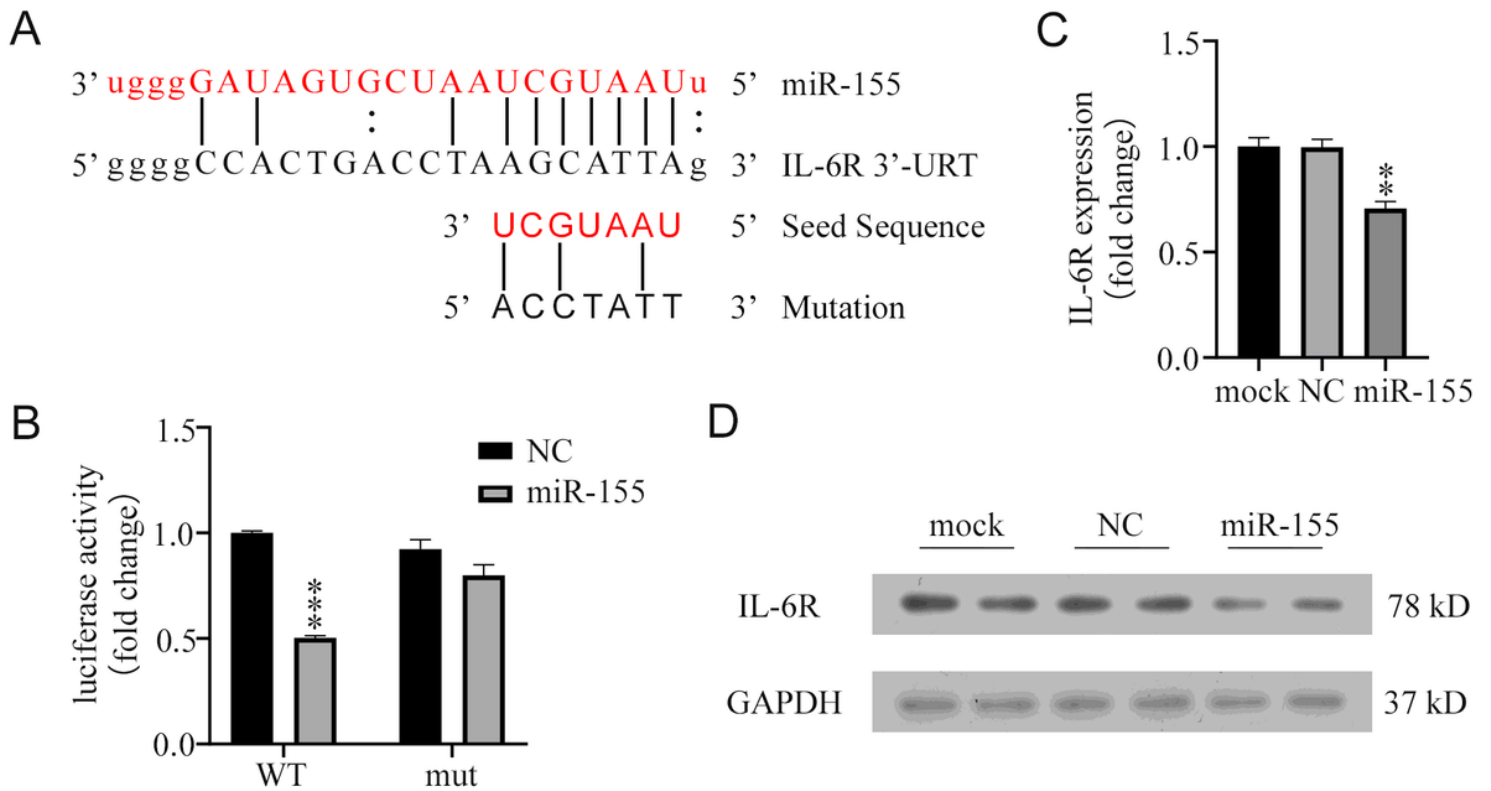


Figure 5

IL-6R as a new target gene of miR-155

A) Bioinformatics analysis suggested that IL-6R is a new target gene of miR-155. B) 20 nM of negative control or miR-155 mimic and 150 ng of pmirGLO plasmid containing WT or 3' -UTR mutation of target gene were co-transfected into HEK293T cells, and dual luciferase activity was detected 48 h later. C) Negative control or miR-155 mimic was transfected into cardiomyocytes at 100 nM, and the mRNA expression of IL-6R in cardiomyocytes was detected by qRT-PCR after 48 h. D) Negative control or miR-155 mimic was transfected into cardiomyocytes at 100 nM, and the IL-6R in cardiomyocytes was analyzed by immunoblotting after 48 h. Each experiment in this figure was replicated more than three times. ** $P < 0.01$, *** $P < 0.001$.

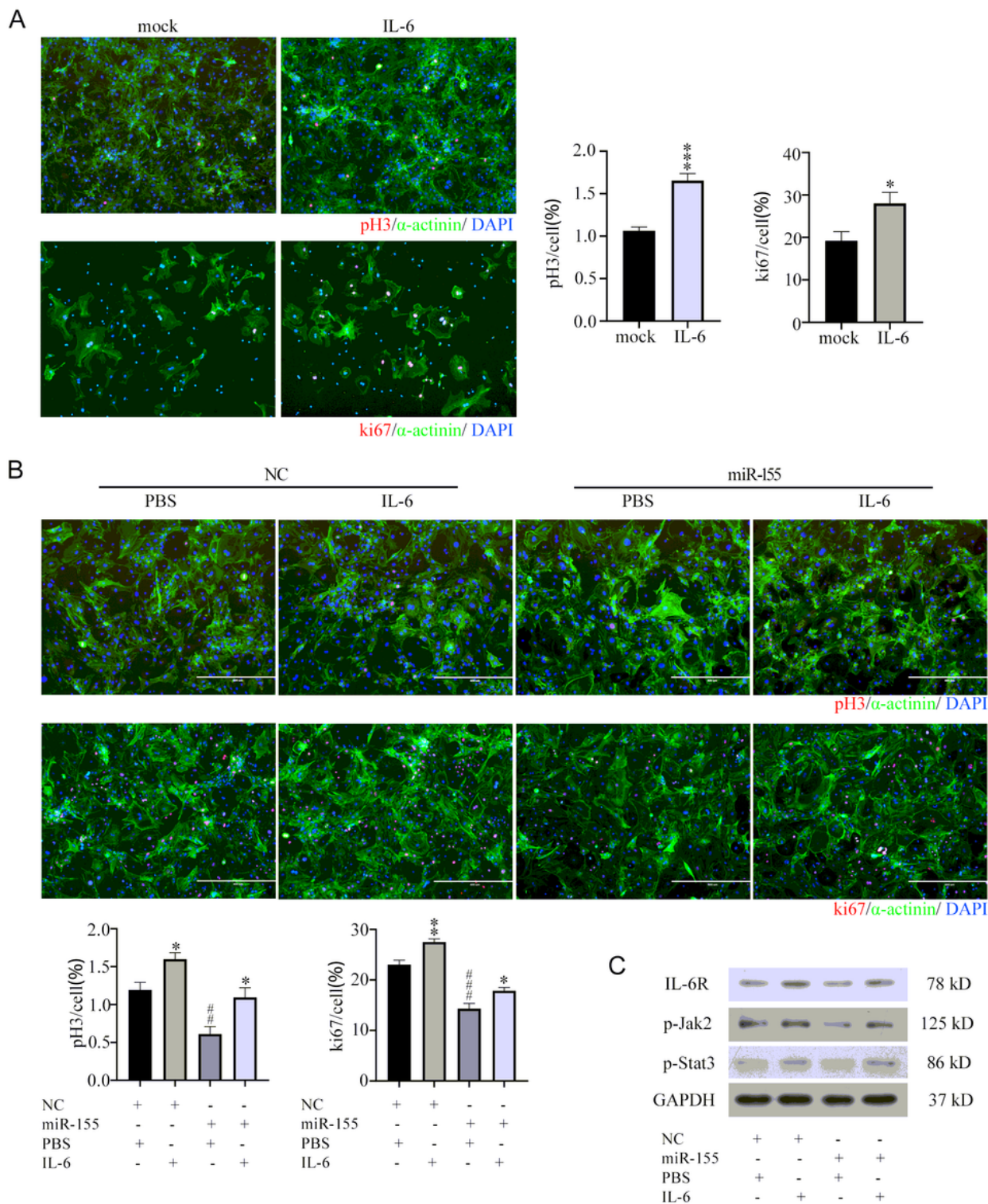


Figure 6

Inhibition of IL6/IL-6R/Jak/Stat pathway by miR-155

A) IL-6 was added to cardiomyocytes at 50 ng/mL for 24 h, and the number of cardiomyocytes labeled with phospho-histone H3 or ki67 was observed by immunocytochemistry. Scale bar: 400 μ m. B) Negative control or miR-155 mimic transfected cardiomyocytes at 100nM for 24 h, and then IL-6 was added at 50

ng/mL for 24 h. The number of cardiomyocytes labeled with phospho-histone H3 or ki67 was observed by immunocytochemistry. Scale bar: 400 μ m. C) Negative control or miR-155 mimic transfected cardiomyocytes at 100 nM for 24 h, and then IL-6 was added for 24 h. Immunoblotting was performed with IL-6R, phospho-Jak2, and phospho-Stat3 antibodies. GAPDH was used as a loading control. Each experiment in this figure was replicated more than three times. * $P < 0.05$, ** $P < 0.01$, *** $P < 0.001$. ## $P < 0.01$, ### $P < 0.001$.

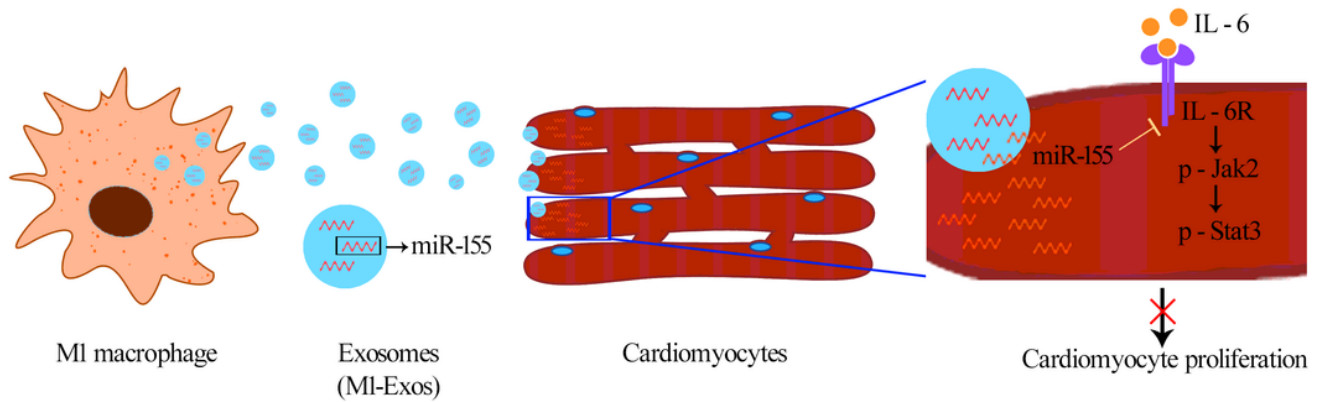


Figure 7

Graphic illustration of the underlying mechanism

When macrophages differentiated into M1 macrophages, they could secrete M1-Exos in large amount. M1-Exos carried miR-155 into cardiomyocytes and targeted IL-6R, thus inhibiting the IL-6R/Jak/Stat pathway, which resulted in the inhibition of cardiomyocyte proliferation.